JBC Papers in Press. Published on June 5, 2015 as Manuscript M115.664813
http://www.jbc.org/cgi/doi/10.1074/jbc.M115.664813

Differences in ATP Generation Via Glycolysis and Oxidative Phosphorylation, and Relationships with Sperm Motility, in Mouse Species

Maximiliano Tourmente[‡], Pilar Villar-Moya[‡], Eduardo Rial[§], and Eduardo R. S. Roldan[‡,1]

[‡]*Reproductive Ecology and Biology Group, Museo Nacional de Ciencias Naturales (CSIC), 28006 Madrid, Spain.*

[§]*Mitochondrial Bioenergetics Research Group, Centro de Investigaciones Biológicas (CSIC), 28040 Madrid, Spain.*

*Running title: *ATP production pathways and sperm performance in mice species*

[1]To whom correspondence should be addressed: E.R.S. Roldan, Reproductive Ecology and Biology Group, Museo Nacional de Ciencias Naturales (CSIC), c/José Gutiérrez Abascal 2, 28006-Madrid, Spain, Tel.: (+34) 914111328 Ext. 1222, Fax: 915645078, E-mail: roldane@mncn.csic.es

Keywords: ATP, glycolysis, respiration, cell metabolism, sperm, mouse

Background: Sperm from mouse species may produce ATP through glycolysis or respiration.
Results: Sperm with high respiration/glycolysis ratio and high reliance on respiration produce more ATP and swim faster.
Conclusion: the usage ratio of ATP production pathways defines sperm motility in mouse species.
Significance: sperm metabolism in mice has evolved ways to produce faster sperm.

ABSTRACT

Mouse sperm produce enough ATP to sustain motility by anaerobic glycolysis and respiration. However, previous studies indicated that an active glycolytic pathway is required to achieve normal sperm function, and identified glycolysis as the main source of ATP to fuel the motility of mouse sperm. All the available evidence has been gathered for the lab mouse, while comparative studies including closely related mouse species have revealed (a) a wide range of variation in sperm motility and ATP production, and (b) that the lab mouse shows comparatively low values in these traits. In this study, we compared the relative reliance on the usage of glycolysis or oxidative phosphorylation as ATP sources for sperm motility between mouse species that exhibit significantly different sperm performance parameters. We found that the sperm of species with higher oxygen consumption/lactate excretion rate ratio were able to produce higher amounts of ATP, achieving higher swimming velocities. Additionally, we show that the species with higher respiration/glycolysis ratio have a higher degree of dependence upon active oxidative phosphorylation. Moreover, we characterize for the first time, two mouse species in which sperm depend on functional oxidative phosphorylation to achieve normal performance. Finally, we discuss that sexual selection through sperm competition could promote adaptations in sperm energetic metabolism tending to increase the usage of oxidative phosphorylation in relation to glycolysis, as this would constitute a more efficient pathway for the generation of ATP (and faster sperm).

INTRODUCTION

Mammalian spermatozoa move forward as a result of thrust generated by the flagellum, a cell component containing the axoneme whose microtubules are associated with large ATPases (dyneins). Sperm motility is directly dependent upon the availability of energy obtained through

ATP hydrolysis (1-3) and accounts for about 70% of total ATP consumption (4). Since spermatozoa are transcriptionally inactive and have a small cytoplasmic volume, their ability to adjust their enzymatic load is very limited (5). In addition, sperm face extensive changes with regards to the availability of oxygen and exogenous metabolic substrates in the different regions of the female tract as they travel to the site of fertilization (2,6,7). Previous studies have hypothesized that mammalian sperm have overcome these limitations by evolving flexible and adaptable metabolic processes that are compartmentalized to specific regions of the cell and function in a localized manner (3,5,8,9). Mammalian sperm rely mainly on two metabolic pathways to produce ATP, namely oxidative phosphorylation (OXPHOS) and anaerobic glycolysis, which are localized to different regions of the cell. On the one hand, OXPHOS takes place in the mitochondria, which are tightly packed in the sperm mid-piece. Numerous studies have provided evidence supporting the role of OXPHOS as the main ATP provider for sperm motility in several mammalian species; in these species, mitochondrial membrane potential and oxygen consumption rate are positively associated with ATP content, proportion of motile sperm and sperm velocity (reviewed in (1-3,10)). On the other hand, glycolysis takes place in the principal piece, which occupies the major part of the flagellum. Several glycolytic enzymes have been identified mainly in the fibrous sheath of the principal piece in mammalian species (11). Because OXPHOS yields more ATP per mol of glucose than glycolysis, mitochondria are abundant in the mid-piece of mammalian sperm, and may use a wider range of substrates (fatty acids, monocarboxylic acids, amino acids), respiration has been historically regarded as the main source of ATP production for sperm motility, relegating glycolysis to a secondary role (12-15). However, there is a wide range of variation among mammalian species with regards to the primary mechanism for ATP production. There are species whose sperm have high respiration rates and cannot support motility with glycolysis alone (boar, horse), species with both high respiration and glycolysis (bull, guinea pig), and others with sperm that rely mainly on glycolysis (human) (9).

In the mouse, numerous experiments on epididymal sperm revealed that both glycolysis and OXPHOS are able to sustain vigorous sperm motility in the presence of their specific substrates (5,10,16-19). Furthermore, mouse sperm are not able to sustain ATP levels and progressive motility when treated with uncoupler agents (17,18) or respiratory inhibitors (10), in glucose free media. However, two studies provided evidence that an active glycolytic pathway is essential for mouse sperm motility and male fertility. Using glyceraldehyde phosphate dehydrogenase (GAPDS) knockout mice (20), or chemical inhibition of glycolysis (21) these studies showed that ATP production and motility were arrested when glycolysis was halted, even if sperm mitochondria were fully functional. The conclusion that glycolysis was essential for mouse sperm was challenged (1-3,10) on the basis that in such studies glycolysis was interrupted after its ATP consuming phase but before its ATP synthesis phase, turning this process into an ATP consumer. Additional studies were carried out using knockout mice for other glycolytic enzymes such as phosphoglycerate kinase 2 (PGK2) (22), enolase 4 (Eno4) (23), and lactate dehydrogenase C (LDHC) (18,24,25). PGK2 catalyzes steps before the ATP-producing phase of the glycolysis, whereas the others are involved in steps during (Eno4) and after (LDHC) the ATP-producing phase. Such studies found that sperm from all these knockout mice have impaired sperm motility and that males experience fertility loss, while maintaining normal mitochondrial activity (at least in the LDHC knockout). In addition, multiple isoforms of glycolytic enzymes in mouse sperm are germ cell-specific, having their expression restricted to spermatogenesis or being produced as sperm-specific splicing variants. These include GAPDHS, PGK2, LDHC, aldolase A (AldoA), Eno4, muscle-type phosphofructokinase (PFKMS), and hexokinase (HK1S) (23,26-32). Many of these enzymes are localized to the principal piece of mouse sperm in close proximity to the axoneme, both in the liposoluble fraction (HK1S, PGK2, Eno4, and LDHC) and in association with the fibrous

sheath (AldoA, GAPDHS, pyruvate kinase, and LDHA) (8,33,34). The unique features of these isozymes may respond to the specificity of the localization of the glycolytic pathway in the principal piece of the sperm flagellum (35). A fully active glycolytic pathway is required for multiple steps in the fertilization cascade, including capacitation-dependent tyrosine phosphorylation, hyperactivated motility, and oocyte penetration (5,17,18,34,36,37). Taken together, evidence suggests that glycolysis is the main source of ATP required to sustain the motility of mouse spermatozoa.

Importantly, knowledge of mouse sperm bioenergetics derives from studies of the laboratory mouse (*Mus musculus*) and, in particular, of a few commonly used mouse strains (CD1, C57BL and 129SvEv). Recent comparative studies in several muroid rodents, have revealed considerable differences in sperm traits and performance within this group of rodents ((38-41); Tourmente et al. unpublished). A strong association was found across species between the content of sperm ATP and both the proportion of motile sperm and sperm swimming velocity, in freshly collected spermatozoa (40) and after a period of incubation (Tourmente et al. unpublished). These results underscore the link between ATP and sperm performance and that sperm from different species may have different demands for efficient fertilization. Interestingly, *M. musculus* exhibited comparatively low ATP content, low percentage of motile sperm and low sperm swimming velocity in relation to other mouse species. This may perhaps relate to the observation that this species, under natural conditions, although under selection for fertilization efficiency, may experience a lower selective pressure for high performance derived from a male-male postcopulatory competitive scenario. Thus, in *M. musculus*, glycolysis, being a less efficient pathway for ATP generation, may suffice for energy production whereas, in other mouse species, sperm that are required to perform at a higher level may need to resort to additional and more efficient ATP-supplying pathways. Therefore, the differences observed between mouse species in an earlier comparative study, and the fact that spermatozoa from *M. musculus* rely highly on glycolysis, prompted the following question: Could the differences in ATP content and sperm swimming velocity between mouse species be related to variation in the usage of different metabolic pathways to generate ATP? In other words, since OXPHOS typically represents a more efficient (per mol of glucose) generation of ATP in comparison to glycolysis, could the higher ATP content and swimming velocity of sperm of other mouse result from a relatively higher reliance on OXPHOS for ATP and sperm motility? A prediction that follows from this question is that species with higher reliance on OXPHOS to generate ATP for sperm motility would suffer a more pronounced decrease in sperm ATP content and swimming performance when OXPHOS is inhibited. The aim of this study was therefore to compare the relative reliance on the usage of OXPHOS and glycolysis as ATP source to sustain sperm motility between mouse species that exhibit significantly different sperm performance parameters.

MATERIALS AND METHODS

Animals and sperm collection

This study focused on three mouse species: the house mouse (*Mus musculus*), from which the majority of laboratory mouse strains are derived, the western Mediterranean mouse (*Mus spretus*), and the steppe mouse (*Mus spicilegus*). These three species represent a closely related monophyletic group with an estimated divergence time of approximately 1.7 million years (42,43). However, comparative studies have revealed notable differences between these species regarding sperm numbers, percentage of motile sperm, swimming velocity and ATP content ((38-41); Tourmente et al. unpublished). Adult males (4-6 months old) of the three species were acquired from the Institut des Sciences de l'Evolution, CNRS-Université Montpellier 2, France. These animals belong to the following wild-derived strains (which have been kept in captivity for only a few generations): *Mus musculus*, strain MPB (from Bialowieza, Poland), *Mus spretus,* strain SEB (from Barcelona, Spain), *Mus spicilegus*, strain ZRU (from Kalomoyevka, Ukraine). Animals were maintained under standard conditions (14 h light - 10 h darkness, 22 - 24ºC), with food and

water provided ad libitum. Each male to be used in this study was housed alone (i.e., in individual cages) for at least two weeks before sperm collection. Males were sacrificed by cervical dislocation and weighed immediately. Testes were then removed and weighed. All procedures followed Spanish Animal Protection Regulation RD1201/2005, which conforms to European Union Regulation 2003/65.

Spermatozoa were collected by placing the caudae epididymides in a Petri dish containing culture medium pre-warmed to 37ºC, and allowing sperm to swim out for 5 min. The medium used was a Hepes-buffered modified Tyrode's medium (mT-H: 131.89 mM NaCl, 2.68 mM KCl, 0.49 mM $MgCl_2.6H_2O$, 0.36 mM $NaH_2PO_4.2H_2O$, 20 mM Hepes, 5.56 mM Glucose, 1.80 mM $CaCl_2$), supplemented with 4mg ml^{-1} fatty acid-free bovine serum albumin (44). In order to remove substrates present in the epididymal fluid, the original sperm suspension was transferred to a tube and centrifuged for 2 minutes at 500 xg, after which the supernatant was removed and the sperm were resuspended in mT-H. Then, sperm concentration was estimated by using a modified Neubauer chamber and adjusted to ~20 $x10^6$ sperm ml^{-1} by adding mT-H. The resulting sperm suspension was transferred to plastic tubes and sperm parameters were assessed immediately. In all procedures large-bore pipette tips were used to minimize damage to sperm membranes. Five individuals of each species were used for each set of experiments, set 1: oxygen consumption rate and extracellular acidification rate measurements, set 2: motility, velocity and ATP content measurements, set 3: lactate excretion rate measurements.

Oxygen consumption rate (OCR) and extracellular acidification rate (ECAR) asessment

An XF24 extracellular flux analyzer (Seahorse Bioscience, North Billerica, MA, USA) was used to measure the real-time oxygen consumption rate (OCR: pmol O_2 min^{-1}) and extracellular acidification rate (ECAR: mPh min^{-1}, an estimate of the rate of lactate release to the medium) of mouse sperm. Since the ECAR measurement method precludes the use of a pH buffer in the medium, an unbuffered mT medium in which Hepes was replaced with NaCl and pH was adjusted at 7.4 at 37º C was used instead of mT-H for sperm collection, dilution and incubation. After sperm concentration was adjusted, 2 $x10^6$ sperm cells were seeded on each of 20 wells of a XF24 plastic microplate which had been previously coated with Concanavalin A to ensure sperm adhesion. Plates were coated by placing 20µl of a 0.5 mg/ml Concanavalin A solution in each well and letting it dry. Four wells were left without cells to preform background corrections. After 1 min, the plate was centrifuged for 2 minutes at 1200 xg. This centrifugation was repeated changing the plate orientation to ensure an even adhesion of cells to the bottom of the well. The supernatant was removed from each well and 500 µl of medium were added per well. Then, the plate was placed in the instrument. All the OCR and ECAR measurements were performed at 37º C under air. Taking account the time required for cell counting, seeding and instrument equilibration, the first OCR and ECAR measurements were taken 44 min after collection of samples. Both OCR and ECAR were recorded for the next 21 min. Subsequently, 1µM carbonyl cyanide-p-trifluoromethoxyphenylhydrazone ("FCCP" group) or mT medium ("control" group) were added to each well to measure maximum and spare OCR (since FCCP acts as an uncoupler of mitochondrial respiration). Measurements continued for 26 min, after which 1µM rotenone and 1µM antimycin A were added to all wells to quantify the mitochondria-independent OCR. OCR and ECAR were monitored for an additional 16 min and the measurement run ended approximately 107 min after sperm collection. A schematic representation of the experimental design is shown in Figure 1a. After the measurement run ended, sperm in each well were fixed by adding 100 µl of 4% formaldehyde solution, they were detached from the bottom of the well (complete detachment was confirmed under the microscope), and counted using a modified Neubauer chamber. The OCR and ECAR values for each well were normalized by the number of sperm present and are reported as amol O_2 min^{-1} $sperm^{-1}$ and npH min^{-1} $sperm^{-1}$. Basal mitochondrial OCR was calculated by subtracting the OCR values obtainedf after the addition of antimycin A and

rotenone from the OCR values of the first 21 min of the experiment. Maximum mitochondrial OCR was calculated by subtracting the OCR values obtained after the addition of antimycin A and rotenone from the OCR values recoreded in the FCCP group in the 26 min after FCCP addition. Spare OCR capacity was calculated by subtracting the basal OCR values from the maximum OCR values. Basal ECAR was calculated averaging the ECAR values obtained in the first 21 min of the experiment.

Sperm motility and swimming velocity
Assessments of these parameters were adjusted to follow the timing of the OCR and ECAR measurements (see Figure 1b). Sperm suspensions (20 x 10^6 sperm ml^{-1} in mT-H) were incubated in plastic tubes at 37º under air during 56 min (corresponding to the third OCR-ECAR measurement), and sperm parameters were recorded (hereafter, "basal" conditions). Subsequently, the suspensions were divided in two aliquots, incubated for another 35 min and either 1µM antimycin A plus 1µM rotenone ("AA + R" group), or an equivalent volume of mT-H ("control" group) were added, coinciding with the second addition of the OCR-ECAR experiment. After 16 min of incubation, sperm parameters were assessed. Sperm motility was evaluated by examining 10 µl of the sperm suspension, placed between a pre-warmed slide and a coverslip, at 100x magnification under phase-contrast optics. The percentage of motile sperm (MOT) was estimated by at least two independent, experienced observers; estimations from the different observers were averaged and rounded to the nearest 5% value. Additionally, the quality (Q) of sperm movement was ranked in a scale from 1 to 5 (from least to most vigorous movement) and a sperm motility index (SMI) was calculated using the following equation: SMI = (Q * 20 + MOT) / 2.
To assess sperm velocity, an aliquot of sperm suspension was diluted to ~5 x 10^6 sperm ml^{-1}, placed in a pre-warmed microscopy chamber with a depth of 20 µm (Leja, Nieuw-Vennep, The Netherlands), and filmed at 40x using a phase contrast microscope connected to a digital video camera (Basler A312fc, Vision Technologies, Glen Burnie, MD, USA). A minimum of 150 sperm trajectories were assessed using a computer assisted sperm analyser (Sperm Class Analyzer v.4.0, Microptic, Barcelona, Spain), and the following velocity parameters were estimated for each trajectory: curvilinear velocity (VCL, µm s^{-1}), straight-line velocity (VSL, µm s^{-1}), average path velocity (VAP, µm s^{-1}), linearity (LIN = VSL/VCL), straightness (STR = VSL/VAP), wobble (WOB = VAP/VCL), amplitude of lateral head displacement (ALH, µm), and beat-cross frequency (BCF, Hz). The final value for these parameters was calculated as the mean of all the individual trajectories for each control or treated sample.

Sperm ATP content
Samples for ATP quantification were obtained at the same time-points described in the previous sub-section (see Figure 1b). Sperm ATP content was measured using a luciferase-based ATP bioluminescent assay kit (Roche, ATP Bioluminescence Assay Kit HS II). A 100 µl-aliquot of diluted sperm suspension was mixed with 100 µl of Cell Lysis Reagent, vortexed and incubated at room temperature for 5 min. The resulting cell lysate was centrifuged at 12,000 xg for 2 min, and the supernatant was recovered and frozen in liquid N_2. Bioluminescence was measured in triplicate in 96-well plates using a luminometer (Synergy HT, Biotek Instruments Inc.). In each well, 50 µl of Luciferase reagent were added to 50 µl of sample (via auto-injection), and, following a 1 s delay, light emission was measured over a 5 s integration period. Standard curves were constructed using solutions containing known concentrations of ATP diluted in mT-H and Cell Lysis Reagent in a proportion equivalent to that of the samples. ATP content was expressed as amol $sperm^{-1}$.

Sperm lactate excretion rate
In order to examine whether the ECAR values obtained using the Seahorse XF24 extracellular flux analyzer mirrored values of lactate excretion or other acidifying compounds, the sperm basal lactate excretion rate (LER) was measured. At 40, 50, 60 and 70 min after swim out, an aliquot of sperm was centrifuged at 2500 x*g* for 2 min and the supernatant was frozen in liquid N_2. Lactate levels in the supernatant (extracellular medium) were determined using a

commercial kit (Lactate Assay Kit K607, BioVision, Mountain View, CA) based on an enzymatic reaction by lactate oxidase and interaction of the product with a probe to produce color. After preparing the reaction mix according to the supplier's instructions, optical density was measured at λ= 570 nm using a microplate reader (Varioskan Flash, Thermo Fisher Scientific Inc.). Standard curves were constructed using solutions containing known concentrations of lactate diluted in mT-H and Cell Lysis Reagent in a proportion equivalent to that of the samples. LER was estimated through linear least squares regression using the four points provided by the measurements and was expressed as amol min^{-1} $sperm^{-1}$.

Data analysis

Principal component analyses for sperm velocity parameters. Since the sperm velocity parameters tend to be highly correlated (39), principal component analyses (PCA) were performed in order to obtain summarized variables to integrate the velocity information. The variables were divided in two groups termed sperm "velocity" (VCL, VSL, VAP) and sperm "trajectory shape" (LIN, STR, WOB, ALH, BCF) and one independent PCA was carried out for each group. The first principal component for the velocity group (VPC1) accounted for 97.5% of the variability in the three summarized variables (VCL, VSL, VAP), while the second principal component (VPC2) only accounted for 2.5%. The values for each of the three sperm velocity descriptors were significantly correlated with VPC1, but showed no significant correlation with VPC2 (data not shown). In the case of the "trajectory shape" group, the first principal component (TPC1) accounted for 88.3% of the variability, while the second principal component (TPC2) represented 8.7%. The values of all the five variables in this group (LIN, STR, WOB, ALH, BCF) were significantly correlated with TPC1, and only ALH and BCF showed a significant correlation with TPC2 (data not shown). Thus, considering the high percentage of variability absorbed by the PC1 in both variable groups, PC1 values for each treatment and species (hereafter referred to "overall sperm velocity" and "overall trajectory shape") were used as our integrated sperm velocity measures.

Length-adjusted metabolic measures. Since larger cells might contain greater quantities of ATP, differences in cell size should be taken into account when testing possible variations in sperm ATP concentration. We calculated the length-adjusted ATP concentration (amol μm^{-1}) as the ratio between the amount of ATP per sperm for each species and its total sperm length (40). Furthermore, since the two metabolic pathways evaluated in this study take place in two different regions of the sperm flagellum, midpiece (OXPHOS) and principal piece (glycolysis), and these regions vary in size between the species evaluated, we chose to proceed in the same way with OCR, ECAR and LER values. Thus, we estimated length-adjusted OCR (amol O_2 min^{-1} μm^{-1}) using midpiece length, and length-adjusted ECAR (npH min^{-1} μm^{-1}) and LER (amol min^{-1} μm^{-1}) using principal piece length. Total sperm length, midpiece length and principal piece length was obtained for the three species (Tourmente et al. unpublished).

Statistical analyses. The effect of membrane decoupling and OXPHOS inhibition on OCR was analyzed with a two-factor repeated-measures ANOVA for each species, using treatment and time as factors (with 3 and 9 levels, respectively). Differences between conditions were analyzed through a post-hoc multiple comparisons test using the Bonferroni correction. Basal values for MOT, SMI, velocity variables and their summarized paremeters, OCR (basal, maximum, and spare), ECAR and LER were compared between species by means of a one factor ANOVA using species as a factor. A post-hoc test (45) was used to determine pairwise differences between species. To evaluate the influence of OXPHOS inhibition in sperm performance parameters, the control and AA + R groups were compared for each species by means of paired t-test. All variables were log_{10}-transformed for statistical purposes, with the exception of percentages MOT, LIN, STR and WOB, which were arcsine-transformed. The statistical analyses were performed using SPSS Statistics (SPSS v.21.0.0.1; SPSS, IBM Corporation, Somers, NY, USA), and InfoStat v.2011p (Grupo

Infostat, Universidad Nacional de Córdoba, Córdoba, Argentina) with α= 0.05.

RESULTS

Interspecific comparison of OCR, lactate production and sperm performance traits

The extracellular flux measurements revealed that sperm oxygen consumption maintained a relatively steady rate in control conditions for the three species throughout the duration of the experiment (Figure 2a, b, c). Moreover, the sperm of the three species responded to the addition of FCCP with a significant increase in OCR, and showed a significant decrease in this parameter under the influence of antimycin A + rotenone in both treatments (control and FCCP) (Figure 2a, b, c). In addition, ECAR values were also stable for the most part of the experiment, showing a slight increase after the addition of antimycin A + rotenone in *Mus musculus* and *Mus spretus* (Figure 2d, e, f).

While the overall pattern of stimulation and inhibition of OCR was similar for the three species, significant quantitative differences were observed. Basal OCR values, both absolute and length-adjusted, were significantly higher in *M. spretus* and *M. spicilegus* than in *M. musculus* (Figure 3a, Table 1). Moreover, after the addition of FCCP, the same significant differences were observed in the maximum OCR (Figure 3b, Table 1) and spare OCR capacity (Figure 3c, Table 1). The average percentage of OCR stimulation caused by the uncoupling of mitochondrial respiration revealed interspecific differences (*Mus musculus*: 211%, *Mus spretus*: 247%, *Mus spicilegus*: 278%), nonetheless, these differences did not reach statistical significance (ANOVA, F= 1.47, p= 0.2714). On the other hand, basal LER (Figure 3d, Table 1) and ECAR (Table 1) values were significantly higher in *M. musculus* than in the other two species, in both their absolute and length-adjusted measures. The remarkable similarity of the interspecific patterns showed by the ECAR and LER measurements (Figure 4) suggests that most of the extracellular acidification recorded in our extracellular flux experiments do correspond to the excretion of lactate by sperm.

In addition, we calculated the OCR/ECAR ratio as a measure of the relative magnitude of OXPHOS vs glycolysis in each species. *M. spretus* and *M. spicilegus* presented a significantly higher OCR/ECAR ratio than *M. musculus* (Figure 5a, Table1). Since OCR and LER measurements were done in different sets of experiments, only an informative mean OCR/LER ratio (mol O_2 consumed / mol lactate excreted) could be calculated per species. The trend of this estimation (*M. musculus*: 1.53 amol O_2 amol lactate^{-1}, *M. spretus*: 5.96 amol O_2 amol lactate^{-1}, *M. spicilegus*: 7.08 amol O_2 amol lactate^{-1}) coincided with the one showed by the OCR/ECAR ratio.

Basal sperm ATP content (Table 1) and length-adjusted ATP concentration (Figure 5b, Table 1) were higher in *M. spretus* and *M. spicilegus* than in *M. musculus*. Previous studies (Tourmente et al. 2013 and unpublished) have reported a significant relation between differences in ATP content and sperm performance in muroid rodents. Our results confirmed these findings since *M. spretus* and *M. spicilegus* showed a higher percentage in motile sperm (Table 1) and higher sperm motility index (Figure 5c, Table 1). Moreover, the three velocity parameters (VCL, VSL and VAP) (Table 1), along with their summarized scores (overall sperm velocity; VPC1) (Figure 5d, Table 1) showed higher values in *M. spretus* and *M. spicilegus* than in *M. musculus*. Finally, when the descriptors of sperm trajectory shape were analyzed, *M. spretus* and *M. spicilegus* showed sperm with more linear and progressive trajectories (higher LIN, STR and WOB), and more frequent (higher BCF) but less pronounced (lower ALH) lateral displacement (Table 1). These differences were also reflected in their summarized scores for these variables (overall trajectory shape; TPC1), which were significantly higher in *M. spretus* and *M. spicilegus* than in *M. musculus* (Table 1).

Effect of OXPHOS inhibition in the sperm of three species of the genus Mus

The inhibition of mitochondrial respiration affected the sperm of the three species in different manner and intensity. Significant differences between the control and AA + R groups are summarized for each species in Table 2. In the case of *Mus musculus* sperm, no

significant differences were registered between groups in any of the ATP values (absolute and length-adjusted) (Figure 6a), motile sperm percentage, SMI (Figure 6b), and the summarized velocity (Figure 6c) and trajectory shape variables (Figure 6d). When analyzing the individual velocity and trajectory shape variables, we only found a significant 6% decrease in the VCL as a result of the inhibition of OXPHOS (Table 2). On the other hand, *M. spretus* and *M. spicilegus* showed significant alterations in sperm motility and energy production as a response of OXPHOS inhibition. In both species, sperm ATP content (both absolute and length-adjusted) (Figure 6a), motile sperm percentage, and SMI (Figure 6b), decreased as a result of the incubation in presence of 1μM antimycin A and 1μM rotenone. However, while *M. spicilegus* sperm decreased both their overall sperm velocity (Figure 6c) and overall trajectory shape (Figure 6d) values under the effect of OXPHOS inhibitors, *M. spretus* sperm only showed significant decreases in the first of the two variables (Figure 6c, d). According with these results, the separate analysis of the sperm velocity and trajectory-shape variables revealed a significant decrease in the eight variables measured for *M. spicilegus* (Table 2), but only in the three variables that composed the overall sperm velocity score (VCL, VSL, and VAP) for *M. spretus* (Table 2). Remarkably, after the incubation under respiration inhibiting conditions, *M. spicilegus* sperm parameters were very similar to those of the *M. musculus* control group (Length adjusted ATP concentration F= 2.85, p= 0.1256; SMI F= 2.39, p= 0.1563; overall sperm velocity F= 0.08, p= 0.7887; overall trajectory shape, F= 0.50, p= 0.4960) (Figure 6).

DISCUSSION

Differences in sperm energetic metabolism translate into variations in sperm ATP production and swimming performance

The results of our study revealed the existence of significant variance in the bioenergetics metabolism of three different species of the genus *Mus*. Our study has in fact two main premises: (a) that the variability in sperm performance seen in species of the genus Mus is a consequence of differences in the usage ratio of two ATP generation pathways (OXPHOS and glycolysis), and (b) that these differences could be adaptations to different levels of sperm competition (since faster sperm are more competitive). In this sense, our analyses showed that the sperm of *Mus musculus* have a lower basal and maximum respiration rate that *M. spretus* and *M. spicilegus*, but excretes lactate to the extracellular medium at a higher rate. Furthermore, these divergences regarding the metabolic pathways usage ratios, translate into variations in sperm ATP content and sperm performance. Thus, in accordance with our hypothesis, the species with higher sperm respiratory activity also showed higher sperm ATP content, percentage of motile cells, sperm motility index, faster sperm velocity, and more linear and progressive trajectories. Previous studies comparing the sperm of hominid (46) and felid (47) species have also found differences in the level of sperm metabolic traits (mitochondrial membrane potential). More specifically, a recent study found significant divergences in the levels of glucose consumption and glycolytic enzymes activity between two strains of laboratory mouse (18). However, in all these cases, the differences that were registered at basal metabolic level did not appear to translate into divergences in sperm performance traits (18,47) or ATP content (18). To our knowledge, the present study is the first to produce evidence relating variations in the usage of sperm metabolic pathways to differences in sperm performance among closely related mammalian species.

Our results indicate that a higher basal rate of OXPHOS could benefit sperm performance by increasing the amount of ATP available for flagellar motility. Moreover, this trend corresponded with a decrease in the rate at which lactate was excreted to the extracellular medium, which would intuitively lead to infer a reduced glycolytic activity in these cells. Yet, this would constitute a somewhat premature conclusion: although sperm function as a highly compartmentalized cell (48), interactions between components of glycolytic and respiratory pathways have been found in the

mouse sperm (17). As an example, the pyruvate dehydrogenase complex (usually located in the mitochondrial matrix), has been detected in the principal piece of hamster sperm (49). Furthermore, the GLUT8 glucose transport facilitator has been found in the mouse sperm midpiece where it is required for the maintenance of mitochondrial membrane potential (50).

Regardless of whether lactate (51-53) or pyruvate (18,34,54) is the primary respiratory substrate entering mouse sperm mitochondria, the composition of the medium used in our experiments made active glycolysis a prerequisite for OXPHOS. While the physiological (*in vivo*) relevance of the uptake by mitochondria of glycolytic products excreted by the principal piece is uncertain, the different regions of the mouse female reproductive tract (vagina, uterus, and oviduct) present relatively high lactate/glucose ratios around the time of ovulation (2,7) that would enable sperm to import sufficient exogenous lactate to fuel OXPHOS (52,53,55,56). Furthermore, when sperm are suspended in seminal plasma, fructose is by far the main metabolic substrate (2). Under these conditions, the ability to incorporate sperm-excreted lactate would enable these cells to produce ATP via both metabolic pathways (OXPHOS and glycolysis). Thus, the onset of OXPHOS using sperm-derived lactate could indeed function to "jump-start" sperm metabolism upon sperm activation when sperm plus seminal plasma enter the vagina.

As a consequence of our experimental setup, the total amount of lactate present in the extracellular medium is the result of the balance between the lactate produced by the glycolytic activity of the cell, and the lactate used as respiratory substrate (possibly after a LDH-catalyzed conversion to pyruvate), making the OCR/LER ratio (the amount of O_2 consumed per mole of lactate excreted) a rather useful measure of the relative usage of each metabolic pathway. Altogether, the comparison of the sperm metabolic output between the three species studied suggests that those sperm in which the products of glycolysis enter the OXPHOS pathway in a higher proportion are able to produce higher amounts of ATP, achieving higher swimming velocities.

The inhibition of OXPHOS affects sperm ATP production and swimming performance in species with high respiratory rates

The inhibition of mitochondrial respiration elicited a decrease of sperm ATP content and sperm performance in the species with high respiration rates (*M. spretus* and *M. spicilegus*), while having no significant effect (beyond a 6% reduction in one velocity parameter) in *M. musculus*. Furthermore, while the sperm of both species with high respiration rates showed a significant reduction of sperm ATP content (-30% in *M. spretus*, -40% in *M. spicilegus*), their swimming performance was affected with different intensity by OXPHOS inhibition. In the case of *M. spretus*, sperm showed a moderate reduction of motility (SMI=-10%) and the variables related to swimming velocity (VCL=-7%, VSL=-11%, VAP=-10%) when OXPHOS was inhibited. A more pronounced decrease in these variables was observed in *Mus spicilegus* sperm (SMI=-25%, VCL=-19%, VSL=-39%, VAP=-30%), in addition to significant variations of the sperm trajectory shape towards less linear trajectories (LIN=-25%, STR=-11%, WOB=-14%) with higher lateral displacements (ALH=20%, BCF=-39%).

The relative importance of OXPHOS vs glycolysis in the production of ATP for mouse sperm motility is still a matter of debate (1-3,57). On the one hand, germ cell-specific variants of genes that encode for OXPHOS related proteins, such as cytochrome *c* (58), succinyl-CoA transferase (59), and pyruvate dehydrogenase (60) have been identified in mouse sperm. Furthermore, male mice knockout for testis-specific cytochrome *c* (16) and choline dehydrogenase (crucial for the maintenance of mitochondrial membrane potential) (61), have diminished motility, ATP levels, and fertility, and mtDNA mutator phenotype strain males are virtually infertile (62). In addition, several studies have shown that laboratory mouse sperm are able to rely solely on respiratory substrates to support motility in the absence of glucose (17,21,37). Notably, this ability is disrupted when glycolysis is inhibited and glucose is also present as a substrate (18-21). On the other hand, glycolysis has been shown to be able to sustain the levels of ATP required for normal motility in

mouse sperm, even after the inhibition of OXPHOS in the presence of oxidative substrates (17,18,20,22). The reliance of murine sperm on active glycolysis to achieve normal sperm motility has been recently explained in terms of metabolic compartmentalization (19): these authors observed that the inhibition of glycolysis, even in sperm supplied with respiratory substrates, promoted a decrease in the bending angle at the distal end of the flagellum. They proposed that, besides producing ATP when provided with glycolysable substrates, glycolytic enzymes located throughout the principal piece (PGK and GAPDH) would catalyze sequential rapid equilibrating reactions constituting an ATP-transferring mechanism from high ATP concentration zones (mitochondria) to low ATP concentration ones (distal flagellum), a process that would not be possible by passive ATP diffusion (63,64).

Our analyses on *M. musculus* sperm appear to confirm this previous evidence since its sperm appear to ignore the effects of OXPHOS inhibition. However, our main result revealed, for the first time, that in other species of the genus *Mus* (*M. spretus* and *M. spicilegus*) sperm depend on a functional respiratory pathway to achieve normal ATP production and motile performance. In addition, our results suggest that the species with more intense respiratory function and higher OCR/LER ratio (*M. spicilegus*) would have a higher degree of reliance upon OXPHOS. On a final note, the differences in the decrease of sperm performance under respiratory inhibition between *M. spretus* and *M. spicilegus* could be explained in terms of compensation between metabolic pathways. Of these two species, only *M. spretus* sperm showed a significant increase in lactate excretion rate after the addition of respiratory inhibitors. Thus, the sperm of *M. spretus* could be (at least partially) compensating for the decrease in ATP levels caused by respiratory inhibition by increasing their glycolytic rate.

Sperm competition as a possible explanation for the evolution of sperm metabolism

The evolution of differences in sperm metabolism between closely related mouse species may be regarded as an adaptive response to selective pressures imposed by sperm competition. Sperm competition is a phenomenon that arises from female promiscuity, in which case, sperm from more than one male would compete to fertilize a given set of ova (65). In the case of muroid rodents, sperm competition has been found to promote a high number of adaptations in sperm traits tending to increase their competitiveness. Comparative studies on this group (which included numerous species of the genus *Mus*) have revealed that species with high levels of sperm competition have higher sperm numbers, percentages of acrosomal integrity, morphologically normal sperm, motile sperm (38), and higher sperm velocity (39,40). In the particular case of sperm velocity, it has been shown to evolve through adaptations in regulatory processes (sequence of ion channels in the sperm tail (41)), and sperm structure (evolution of protamines and head morphology (39,66)). More importantly, previous results from our group indicate that the increase in sperm swimming velocity in species with high sperm competition levels is mainly related to an elevation in sperm ATP production ((40); Tourmente et al. unpublished).

Sperm competition levels in mammals can be inferred by measuring the mass of the testes of a species in relation to its body mass (a reliable indicator of sperm competition level (67)). The inferred sperm competition levels for *M. musculus*, *M. spretus* and *M. spicilegus* are respectively low (testes mass = 0.63% of body mass), intermediate (1.73%), and high (2.82%), in comparison with other species of the genus *Mus* (38). Although a higher number of species may be required for a correlational analysis between sperm competition and sperm metabolic features, the trend observed in the present study is clear: high levels of sperm competition promote an increase in the ATP production capabilities of mouse sperm, and the species with higher sperm competition level present higher OXPHOS activity. Altogether, this evidence would suggest that sperm competition could promote adaptations in sperm energetic metabolism tending to increase the usage of OXPHOS in relation to glycolysis, since it

would constitute a more efficient pathway for the generation of high amounts of ATP.

ACKNOWLEDGEMENTS

We thank Juan Antonio Rielo for supervising animal facilites and Esperanza Navarro for animal care at the Museo Nacional de Ciencias Naturales in Madrid. We are also grateful to F. Bonhomme and A. Orth (Institut des Sciences de l'Evolution, CNRS-Universite´ Montpellier 2) who facilitated the acquisition of mice. This study was supported by the Spanish Ministry of Economy and Competitiveness. M.T. holds a "Juan de la Cierva" postdoctoral fellowship from the Ministry of Economy and Competitiveness whereas Pilar Villar-Moya was the recipient of a JAE-Tec training scholarship. The funders had no role in study design, data collection and analysis, decision to publish, or preparation of the manuscript.

REFERENCES

1. Ford, W. C. (2006) Glycolysis and sperm motility: does a spoonful of sugar help the flagellum go round? *Hum Reprod Update* **12**, 269-274.
2. Ruiz-Pesini, E., Díez-Sánchez, C., López-Pérez, M. J., and Enríquez, J. A. (2007) The Role of the Mitochondrion in Sperm Function: Is There a Place for Oxidative Phosphorylation or Is This a Purely Glycolytic Process? *Curr Top Dev Biol* **77**, 3-19.
3. Storey, B. T. (2008) Mammalian sperm metabolism: oxygen and sugar, friend and foe. *Int J Dev Biol* **52**, 427-437.
4. Bohnensack, R., and Halangk, W. (1986) Control of respiration and of motility in ejaculated bull spermatozoa. *Biochim Biophys Acta* **850**, 72-79.
5. Travis, A. J., Jorgez, C. J., Merdiushev, T., Jones, B. H., Dess, D. M., Diaz-Cueto, L., Storey, B. T., Kopf, G. S., and Moss, S. B. (2001) Functional relationships between capacitation-dependent cell signaling and compartmentalized metabolic pathways in murine spermatozoa. *J Biol Chem* **276**, 7630-7636.
6. Gardner, D. K., and Leese, H. J. (1990) Concentrations of nutrients in mouse oviduct fluid and their effects on embryo development and metabolism in vitro. *J Reprod Fertil* **88**, 361-368.
7. Harris, S. E., Gopichandran, N., Picton, H. M., Leese, H. J., and Orsi, N. M. (2005) Nutrient concentrations in murine follicular fluid and the female reproductive tract. *Theriogenology* **64**, 992-1006.
8. Miki, K. (2007) Energy metabolism and sperm funtion. in *Spermatology* (Roldan, E. R. S., and Gomendio, M. eds.), Nottingham University Press, Nottingham. pp 309-325
9. Cummins, J. M. (2009) Sperm motility and energetics. in *Sperm biology, an evolutionary perspective* (Birkhead, T. R., Hosken, D. J., and Pitnick, S. eds.), Academic Press, San Diego, CA. pp 185-206
10. Pasupuleti, V. (2007) *Msc. Thesis: Role of glycolysis and representation in sperm metabolism and motility.* MSc, Kent State University
11. Turner, R. M. (2006) Moving to the beat: a review of mammalian sperm motility regulation. *Reprod Fertil Dev* **18**, 25-38.
12. Van Dop, C., Hutson, S. M., and Lardy, H. A. (1977) Pyruvate metabolism in bovine epididymal spermatozoa. *J Biol Chem* **252**, 1303-1308
13. Hammerstedt, R. H., and Lardy, H. A. (1983) The effect of substrate cycling on the ATP yield of sperm glycolysis. *J Biol Chem* **258**, 8759-8768
14. Gopalkrishnan, K., Padwal, V., D'Souza, S., and Shah, R. (1995) Severe asthenozoo-spermia: a structural and functional study. *Int J Androl* **18**, 67-74.
15. Ferramosca, A., Focarelli, R., Piomboni, P., Coppola, L., and Zara, V. (2008) Oxygen uptake by mitochondria in demembranated human spermatozoa: a reliable tool for the evaluation of sperm respiratory efficiency. *Int J Androl* **31**, 337-345.

16. Narisawa, S., Hecht, N. B., Goldberg, E., Boatright, K. M., Reed, J. C., and Millan, J. L. (2002) Testis-Specific Cytochrome c-Null Mice Produce Functional Sperm but Undergo Early Testicular Atrophy. *Mol Cell Biol* **22**, 5554-5562.
17. Goodson, S. G., Qiu, Y., Sutton, K. A., Xie, G., Jia, W., and O'Brien, D. A. (2012) Metabolic substrates exhibit differential effects on functional parameters of mouse sperm capacitation. *Biol Reprod* **87**, 75.
18. Odet, F., Gabel, S., London, R. E., Goldberg, E., and Eddy, E. M. (2013) Glycolysis and mitochondrial respiration in mouse LDHC-null sperm. *Biol Reprod* **88**, 95.
19. Takei, G. L., Miyashiro, D., Mukai, C., and Okuno, M. (2014) Glycolysis plays an important role in energy transfer from the base to the distal end of the flagellum in mouse sperm. *J Exp Biol* **217**, 1876-1886.
20. Miki, K., Qu, W., Goulding, E. H., Willis, W. D., Bunch, D. O., Strader, L. F., Perreault, S. D., Eddy, E. M., and O'Brien, D. A. (2004) Glyceraldehyde 3-phosphate dehydrogenase-S, a sperm-specific glycolytic enzyme, is required for sperm motility and male fertility. *Proc Natl Acad Sci U S A* **101**, 16501-16506.
21. Mukai, C., and Okuno, M. (2004) Glycolysis plays a major role for adenosine triphosphate supplementation in mouse sperm flagellar movement. *Biol Reprod* **71**, 540-547.
22. Danshina, P. V., Geyer, C. B., Dai, Q., Goulding, E. H., Willis, W. D., Kitto, G. B., McCarrey, J. R., Eddy, E. M., and O'Brien, D. A. (2010) Phosphoglycerate kinase 2 (PGK2) is essential for sperm function and male fertility in mice. *Biol Reprod* **82**, 136-145.
23. Nakamura, N., Dai, Q., Williams, J., Goulding, E. H., Willis, W. D., Brown, P. R., and Eddy, E. M. (2013) Disruption of a spermatogenic cell-specific mouse enolase 4 (eno4) gene causes sperm structural defects and male infertility. *Biol Reprod* **88**, 90.
24. Odet, F., Duan, C., Willis, W. D., Goulding, E. H., Kung, A., Eddy, E. M., and Goldberg, E. (2008) Expression of the gene for mouse lactate dehydrogenase C (Ldhc) is required for male fertility. *Biol Reprod* **79**, 26-34.
25. Odet, F., Gabel, S. A., Williams, J., London, R. E., Goldberg, E., and Eddy, E. M. (2011) Lactate dehydrogenase C and energy metabolism in mouse sperm. *Biol Reprod* **85**, 556-564.
26. Boer, P. H., Adra, C. N., Lau, Y. F., and McBurney, M. W. (1987) The testis-specific phosphoglycerate kinase gene pgk-2 is a recruited retroposon. *Mol Cell Biol* **7**, 3107-3112.
27. Li, S. S., O'Brien, D. A., Hou, E. W., Versola, J., Rockett, D. L., and Eddy, E. M. (1989) Differential activity and synthesis of lactate dehydrogenase isozymes A (muscle), B (heart), and C (testis) in mouse spermatogenic cells. *Biol Reprod* **40**, 173-180.
28. Welch, J. E., Schatte, E. C., O'Brien, D. O., and Eddy, E. M. (1992) Expression of a Glyceraldehyde 3-phosphate dehydrogenase gene specific to mouse spermatogenic cells. *Biol Reprod* **46**, 869-878.
29. Mori, C., Nakamura, N., Welch, J. E., Gotoh, H., Goulding, E. H., Fujioka, M., and Eddy, E. M. (1998) Mouse spermatogenic cell–specific type 1 Hexokinase (mHk1-s) transcripts are expressed by alternative splicing from the mHk1 gene and the HK1-S protein is localized mainly in the sperm tail. *Mol Reprod Dev* **49**, 374-385.
30. Bunch, D. O., Welch, J. E., Magyar, P. L., Eddy, E. M., and O'Brien, D. A. (1998) Glyceraldehyde 3-phosphate dehydrogenase-S protein distribution during mouse spermatogenesis. *Biol Reprod* **58**, 834-841.
31. Vemuganti, S. A., Bell, T. A., Scarlett, C. O., Parker, C. E., de Villena, F. P., and O'Brien, D. A. (2007) Three male germline-specific aldolase A isozymes are generated by alternative splicing and retrotransposition. *Dev Biol* **309**, 18-31.
32. Nakamura, N., Mori, C., and Eddy, E. M. (2010) Molecular complex of three testis-specific isozymes associated with the mouse sperm fibrous sheath: hexokinase 1, phosphofructokinase M, and glutathione S-transferase mu class 5. *Biol Reprod* **82**, 504-515.
33. Krisfalusi, M., Miki, K., Magyar, P. L., and O'Brien, D. A. (2006) Multiple glycolytic enzymes are tightly bound to the fibrous sheath of mouse spermatozoa. *Biol Reprod* **75**, 270-278.

34. Tang, H., Duan, C., Bleher, R., and Goldberg, E. (2013) Human lactate dehydrogenase A (LDHA) rescues mouse Ldhc-null sperm function. *Biol Reprod* **88**, 96.
35. Eddy, E. M., Toshimori, K., and O'Brien, D. A. (2003) Fibrous sheath of mammalian spermatozoa. *Microsc Res Tech* **61**, 103-115.
36. Urner, F., Leppens-Luisier, G., and Sakkas, D. (2001) Protein Tyrosine phosphorylation in sperm during gamete interaction in the mouse: the influence of Glucose. *Biol Reprod* **64**, 1350-1357.
37. Tanaka, H., Takahashi, T., Iguchi, N., Kitamura, K., Miyagawa, Y., Tsujimura, A., Matsumiya, K., Okuyama, A., and Nishimune, Y. (2004) Ketone bodies could support the motility but not the acrosome reaction of mouse sperm. *Int J Androl* **27**, 172-177.
38. Gomez Montoto, L., Magana, C., Tourmente, M., Martin-Coello, J., Crespo, C., Luque-Larena, J. J., Gomendio, M., and Roldan, E. R. S. (2011) Sperm competition, sperm numbers and sperm quality in muroid rodents. *PLoS One* **6**, e18173.
39. Gomez Montoto, L., Varea Sanchez, M., Tourmente, M., Martin-Coello, J., Luque-Larena, J. J., Gomendio, M., and Roldan, E. R. S. (2011) Sperm competition differentially affects swimming velocity and size of spermatozoa from closely related muroid rodents: head first. *Reproduction* **142**, 819-830.
40. Tourmente, M., Rowe, M., González-Barroso, M. M., Rial, E., Gomendio, M., and Roldan, E. R. S. (2013) Postcopulatory sexual selection increases ATP content in rodent spermatozoa. *Evolution* **67**, 1838-1846.
41. Vicens, A., Tourmente, M., and Roldan, E. R. S. (2014) Structural evolution of CatSper1 in rodents is influenced by sperm competition, with effects on sperm swimming velocity. *BMC Evol Biol* **14**, 106.
42. Suzuki, H., Nunome, M., Kinoshita, G., Aplin, K., Vogel, P., Kryukov, A. P., Jin, M. L., Han, S. H., Maryanto, I., Tsuchiya, K., Ikeda, H., Shiroishi, T., Yonekawa, H., and Moriwaki, K. (2013) Evolutionary and dispersal history of Eurasian house mice Mus musculus clarified by more extensive geographic sampling of mitochondrial DNA. *Heredity* **111**, 375-390.
43. Cazaux, B., Catalan, J., Justy, F., Escude, C., Desmarais, E., and Britton-Davidian, J. (2013) Evolution of the structure and composition of house mouse satellite DNA sequences in the subgenus Mus (Rodentia: Muridea): a cytogenomic approach. *Chromosoma* **122**, 209-220.
44. Shi, Q., and Roldan, E. R. S. (1995) Bicarbonate/CO2 is not required for zona pellucida- or progesterone-induced acrosomal exocytosis of mouse spermatozoa but is essential for capacitation. *Biol Reprod* **52**, 540-546.
45. Di Rienzo, J. A., Guzmán, A. W., and Casanoves, F. (2002) A multiple comparisons method based on the distribution of the root node distance of a binary tree. *Journal of Agricultural, Biological and Environment Statistics* **7**, 129-142
46. Anderson, M. J., Chapman, S. J., Videan, E. N., Evans, E., Fritz, J., Stoinski, T. S., Dixson, A. F., and Gagneux, P. (2007) Functional evidence for differences in sperm competition in humans and chimpanzees. *Am J Phys Anthropol* **134**, 274-280.
47. Terrell, K. A., Wildt, D. E., Anthony, N. M., Bavister, B. D., Leibo, S. P., Penfold, L. M., Marker, L. L., and Crosier, A. E. (2011) Oxidative phosphorylation is essential for felid sperm function, but is substantially lower in cheetah (Acinonyx jubatus) compared to domestic cat (Felis catus) ejaculate. *Biol Reprod* **85**, 473-481.
48. Mukai, C., and Travis, A. J. (2012) What sperm can teach us about energy production. *Reprod Domest Anim* **47**, 164-169.
49. Mitra, K., Rangaraj, N., and Shivaji, S. (2005) Novelty of the pyruvate metabolic enzyme dihydrolipoamide dehydrogenase in spermatozoa: correlation of its localization, tyrosine phosphorylation, and activity during sperm capacitation. *J Biol Chem* **280**, 25743-25753.
50. Gawlik, V., Schmidt, S., Scheepers, A., Wennemuth, G., Augustin, R., Aumuller, G., Moser, M., Al-Hasani, H., Kluge, R., Joost, H. G., and Schurmann, A. (2008) Targeted disruption of Slc2a8 (GLUT8) reduces motility and mitochondrial potential of spermatozoa. *Molecular membrane biology* **25**, 224-235.

51. Gallina, F. G., Gerez de Burgos, N. M., Burgos, C., Coronel, C. E., and Blanco, A. (1994) The lactate/pyruvate shuttle in spermatozoa: operation *in vitro*. *Arch Biochem Biophys* **308**, 515-519.
52. Burgos, C., Maldonado, C., Gerez de Burgos, N. M., Aoki, A., and Blanco, A. (1995) Intracellular localization of the testicular and sperm-specific lactate dehydrogenase isozyme C4 in mice. *Biol Reprod* **53**, 84-92.
53. Montamat, E. E., Vermouth, N. T., and Blanco, A. (1988) Subcellular localization of branched-chain amino acid aminotransferase and lactate dehydrogenase C4 in rat and mouse spermatozoa. *Biochem J* **255**, 1053-1056
54. Mannowetz, N., Wandernoth, P. M., and Wennemuth, G. (2012) Glucose is a pH-dependent motor for sperm beat frequency during early activation. *PLoS One* **7**, e41030.
55. Garcia, C. K., Brown, M. S., Pathak, R. K., and Goldstein, J. L. (1995) cDNA cloning of MCT2, a second monocarboxylate transporter expressed in different cells than MCT1. *J Biol Chem* **270**, 1843-1849
56. Boussouar, F., Mauduit, C., Tabone, E., Pellerin, L., Magistretti, P. J., and Benahmed, M. (2003) Developmental and hormonal regulation of the monocarboxylate transporter 2 (MCT2) expression in the mouse germ cells. *Biol Reprod* **69**, 1069-1078.
57. Amaral, A., Lourenco, B., Marques, M., and Ramalho-Santos, J. (2013) Mitochondria functionality and sperm quality. *Reproduction* **146**, R163-174.
58. Hennig, B. (1975) Change of cytochrome c structure during development of the mouse. *European Journal of Biochemistry* **55**, 167-183
59. Tanaka, H., Iguchi, N., Miyagawa, I., Koga, M., Kohroki, J., and Nishimune, Y. (2003) Differential expression of succinyl CoA transferase (SCOT) genes in somatic and germline cells of the mouse testis. *Int J Androl* **26**, 52-56
60. Gerez de Burgos, N. M., Gallina, F. G., Burgos, C., and Blanco, A. (1994) Effect of L-malate on pyruvate dehydrogenase activity of spermatozoa. *Arch Biochem Biophys* **308**, 520-524
61. Johnson, A. R., Craciunescu, C. N., Guo, Z., Teng, Y. W., Thresher, R. J., Blusztajn, J. K., and Zeisel, S. H. (2010) Deletion of murine choline dehydrogenase results in diminished sperm motility. *FASEB J* **24**, 2752-2761.
62. Trifunovic, A., Wredenberg, A., Falkenberg, M., Spelbrink, J. N., Rovio, A. T., Bruder, C. E., Bohlooly, M., Gildöf, S., Oldfors, A., Wibom, R., Törnell, J., Jacobs, H. T., and Larsson, N. G. (2004) Premature ageing in mice expressing defective mitochondrial DNA polymerase. *Nature* **429**, 417-423.
63. Takao, D., and Kamimura, S. (2008) FRAP analysis of molecular diffusion inside sea-urchin spermatozoa. *J Exp Biol* **211**, 3594-3600.
64. Nevo, A. C., and Rikmenspoel, R. (1970) Diffusion of ATP in sperm flagella. *J Theor Biol* **26**, 11-18
65. Parker, G. A. (1970) Sperm competition and its evolutionary consequences in insects. *Biol Rev* **45**, 525-567.
66. Lüke, L., Vicens, A., Tourmente, M., and Roldan, E. R. (2014) Evolution of protamine genes and changes in sperm head phenotype in rodents. *Biol Reprod* **90**, 67.
67. Soulsbury, C. D. (2010) Genetic patterns of paternity and testes size in mammals. *PLoS One* **5**, e9581.

FIGURE LEGENDS

Figure 1. Schematic representation of the experiments carried out. (a) Sperm oxygen consumption (OCR: pmol O_2 min^{-1}) and extracellular acidification (ECAR: mPh min^{-1}) rates measurements using the XF24 extracellular flux analyzer (Seahorse Bioscience, North Billerica, MA, USA). (b) Sperm motility, velocity and trajectory shape parameters, ATP content and lactate excretion rate measurements. Control: medium added to the sperm suspension. FCCP: Carbonyl cyanide-p-trifluoromethoxyphenylhydrazone (final

concentration= 1µM) added to the sperm suspension. AA + R: antimycin A (final concentration= 1µM) and rotenone (final concentration= 1µM) added to the sperm suspension.

Figure 2. Oxygen consumption rate (OCR) (a, b, c) and extracellular acidification rate (ECAR) (d, e, f) in three mouse species. (a, d) *Mus musculus*. (b, e) *Mus spretus*. (c, f) *Mus spicilegus*. Treatments: Control (white dots, dashed arrows, medium added in the first addition), and FCCP (black dots, continuous arrow, 1 µM FCCP added in the first addition). Additions are indicated with a grey line: FCCP= Carbonyl cyanide-p-trifluoromethoxyphenylhydrazone (final concentration= 1µM), AA + R= antimycin A (final concentration= 1µM) and rotenone (final concentration= 1µM). *F* and *p* values correspond to repeated measures ANOVAs using treatment, time, and their interaction as factors. Asterisks indicate significant differences ($p< 0.05$) between treatments for the same time. Arrows indicate significant differences ($p< 0.05$) between times for the same treatment.

Figure 3. Comparison of sperm metabolic pathways rates between *M. musculus*, *M. spretus* and *M. spicilegus*. Squares represent averages from a least 5 males per species, whiskers represent SE. (a) Length-adjusted basal oxygen consumption rate. (b) Length-adjusted maximum oxygen consumption rate. (c) Length-adjusted spare oxygen consumption rate. (d) Length-adjusted basal lactate excretion rate. Different letters indicate significant differences ($p< 0.05$) between species in a parametric post-hoc test. OCR: oxygen consumption rate. LER: lactate excretion rate.

Figure 4. Comparison of sperm extracellular acidification and lactate production rates between *M. musculus*, *M. spretus* and *M. spicilegus*. Squares represent averages from a least 5 males per species, whiskers represent SE. (a) Basal extracellular acidification rate. (b) Basal lactate production rate. Different letters indicate significant differences ($p< 0.05$) between species in a parametric post-hoc test. ECAR: extracellular acidification rate. LER lactate production rate.

Figure 5. Comparison of sperm metabolic pathways usage, ATP content and motile performance between *M. musculus*, *M. spretus* and *M. spicilegus*. Squares represent averages from a least 5 males per species, whiskers represent SE. (a) Ratio between basal oxygen consumption rate and basal extracellular acidification rate. (b) Length-adjusted ATP concentration. (c) Sperm motility index. (d) Overall sperm velocity. Different letters indicate significant differences ($p< 0.05$) between species in a parametric post-hoc test. OCR: oxygen consumption rate. ECAR: extracellular acidification rate. VPC1: first principal component of a principal component analysis using VCL, VAP and VSL.

Figure 6. Effect of OXPHOS inhibition on sperm ATP content and motile performance in *M. musculus*, *M. spretus* and *M. spicilegus*. Bars represent averages from a least 5 males per species, whiskers represent SE. White bars: control. Black bars: antimycin A 1µM + rotenone 1µM. (a) Length-adjusted ATP concentration. (b) Sperm motility index. (c) Overall sperm velocity. (d) Overall trajectory shape. Asterisks indicate significant differences ($p< 0.05$) between treatments for the same species (repeated measures ANOVA). VPC1: first principal component of a PCA using VCL, VAP and VSL. TPC1: first principal component of a PCA using LIN, STR, WOB, ALH and BCF.

Table 1. Comparison of basal sperm traits between *M. musculus*, *M. spretus* and *M. spicilegus*. Values represent average from a least 5 males per species. *F* and *p* values correspond to one way ANOVAs using species as a factor. OCR: oxygen consumption rate. ECAR: extracellular acidification rate. LER: lactate excretion rate. L. a.: lenght-adjusted. VPC1: velocity principal component 1. TPC1: trajectory shape principal component 1. Significant differences between species ($p < 0.05$) are shown in bold.

Variables	*M. musculus*	*M. spretus*	*M. spicilegus*	*F*	*p*
Body mass (g)	21.58	19.03	18.43	-	-
Testes mass (g)	0.13	0.31	0.47	-	-
Total sperm numbers (x 10^6)	32.67	85.76	117.37	-	-
Basal OCR (amol O_2 min^{-1} $sperm^{-1}$)	157.51a	205.31b	261.03b	6.19	0.0158
Maximum OCR (amol O_2 min^{-1} $sperm^{-1}$)	324.63a	547.22b	639.12b	13.63	0.0011
Spare OCR (amol O_2 min^{-1} $sperm^{-1}$)	153.63a	342.33b	388.71b	15.64	0.0006
L. a. basal OCR (amol O_2 min^{-1} $sperm^{-1}$ μm^{-1})	6.72a	10.25b	13.38b	11.73	0.0019
L. a. maximum OCR (amol O_2 min^{-1} $sperm^{-1}$ μm^{-1})	13.86a	27.32b	32.76b	22.43	0.0001
L. a. spare OCR (amol O_2 min^{-1} $sperm^{-1}$ μm^{-1})	6.56a	17.09b	19.93b	22.28	0.0001
Basal ECAR (npH min^{-1} $sperm^{-1}$)	17.07b	7.58a	9.72a	18.56	0.0003
Basal LER (amol lactate min^{-1} $sperm^{-1}$)	102.71b	34.47a	36.85a	6.67	0.0113
L. a. basal ECAR (npH min^{-1} $sperm^{-1}$ μm^{-1})	0.19b	0.09a	0.13a	13.37	0.0011
L. a. basal LER (amol lactate min^{-1} $sperm^{-1}$ μm^{-1})	1.09b	0.4a	0.48a	5.16	0.0242
OCR/ECAR ratio (amol O_2 npH^{-1})	9.27a	26.88b	27.28b	151.09	<0.0001
ATP content (amol $sperm^{-1}$)	104.81a	275.6b	253.1b	17.03	0.0003
L. a. ATP concentration (amol $sperm^{-1}$ μm^{-1})	0.86a	2.54b	2.55b	22.79	0.0001
Percentage of motile sperm (%)	64a	83b	83b	21.31	0.0001
Sperm motility index	66a	86.5b	86.5b	32.94	<0.0001
Curvilinear velocity (μm s^{-1})	177.21a	254.02c	228.13b	115.00	<0.0001
Straight-line velocity (μm s^{-1})	84.47a	164.14b	168.78b	139.18	<0.0001
Average path velocity (μm s^{-1})	109.03a	181.53b	176.17b	163.73	<0.0001
Linearity	0.47a	0.66b	0.71c	77.78	<0.0001
Straightness	0.75a	0.92b	0.92b	99.80	<0.0001
Wobble	0.62a	0.71b	0.77c	57.11	<0.0001
Lateral amplitude of head displacement (μm)	5.35c	4.91b	4.53a	51.88	<0.0001
Beat-cross frequency (Hz)	9.5a	21.06c	17.51b	261.75	<0.0001
Overall sperm velocity (VPC1)	-1.45a	2.23b	1.74b	162.48	<0.0001
Overall trajectory shape (TPC1)	-1.6a	2.18b	3.12c	106.45	<0.0001

Table 2. Effect of OXPHOS inhibition in the sperm traits of *M. musculus* , *M. spretus* and *M. spicilegus* . Values represent averages of 5 males per species. *t* and *p* values correspond to a paired *t*-test using Treatment as a factor. AA + R group: antimycin A 1μM + rotenone 1μM was added to the sperm suspension. Control group: an equivalent volume of mT-H was added to the sperm suspension. L. a.: length-adjusted. VPC1: velocity principal component 1. TPC1: trajectory shape principal component 1. Significant differences between treatments (p< 0.05) are shown in bold.

Variables	Treatment	*M. musculus*	*t*	*p*	*M. spretus*	*t*	*p*	*M. spicilegus*	*t*	*p*
ATP content (amol sperm^{-1})	Control	90.01	0.80	0.4674	192.46	6.06	**0.0037**	165.30	4.44	**0.0114**
	AA + R	103.07			133.54			98.00		
L.a. ATP concentration (amol sperm^{-1} μm^{-1})	Control	0.74	0.80	0.4674	1.78	6.06	**0.0037**	1.66	4.44	**0.0114**
	AA + R	0.85			1.23			0.99		
Percentage of motile sperm (%)	Control	44.00	2.37	0.0770	72.00	4.83	**0.0084**	71.00	7.06	**0.0021**
	AA + R	34.00			58.00			52.00		
Sperm motility index	Control	51.00	1.66	0.1713	77.00	3.33	**0.0291**	74.50	8.54	**0.0010**
	AA + R	47.00			69.00			56.00		
Curvilinear velocity (μm s^{-1})	Control	176.82	2.90	**0.0442**	241.87	3.55	**0.0239**	210.46	4.80	**0.0087**
	AA + R	165.83			225.56			171.01		
Straight-line velocity (μm s^{-1})	Control	81.85	1.84	0.1397	141.48	3.39	**0.0275**	137.73	9.36	**0.0007**
	AA + R	69.56			126.05			83.90		
Average path velocity (μm s^{-1})	Control	106.65	1.98	0.1188	159.66	3.94	**0.0169**	153.99	8.40	**0.0011**
	AA + R	96.12			144.01			107.58		
Linearity	Control	0.46	1.29	0.2662	0.57	1.45	0.2196	0.65	8.87	**0.0009**
	AA + R	0.42			0.56			0.49		
Straightness	Control	0.74	1.41	0.2326	0.86	0.80	0.4679	0.87	7.44	**0.0017**
	AA + R	0.70			0.86			0.77		
Wobble	Control	0.61	0.93	0.4063	0.66	1.65	0.1746	0.73	9.82	**0.0006**
	AA + R	0.59			0.64			0.63		
Lateral amplitude of head displacement (μm)	Control	5.46	0.28	0.7917	5.25	0.62	0.5687	4.80	5.93	**0.0041**
	AA + R	5.44			5.21			5.75		
Beat-cross frequency (Hz)	Control	9.15	2.43	0.0722	18.67	0.27	0.7991	14.82	6.79	**0.0025**
	AA + R	7.83			18.74			9.05		
Overall sperm velocity (VPC1)	Control	-1.57	2.15	0.0982	1.42	3.86	**0.0182**	0.83	9.24	**0.0008**
	AA + R	-2.33			0.75			-1.63		
Overall trajectory shape (TPC1)	Control	-1.95	1.28	0.2705	0.56	0.82	0.4558	1.69	7.64	**0.0016**
	AA + R	-2.60			0.37			-1.77		

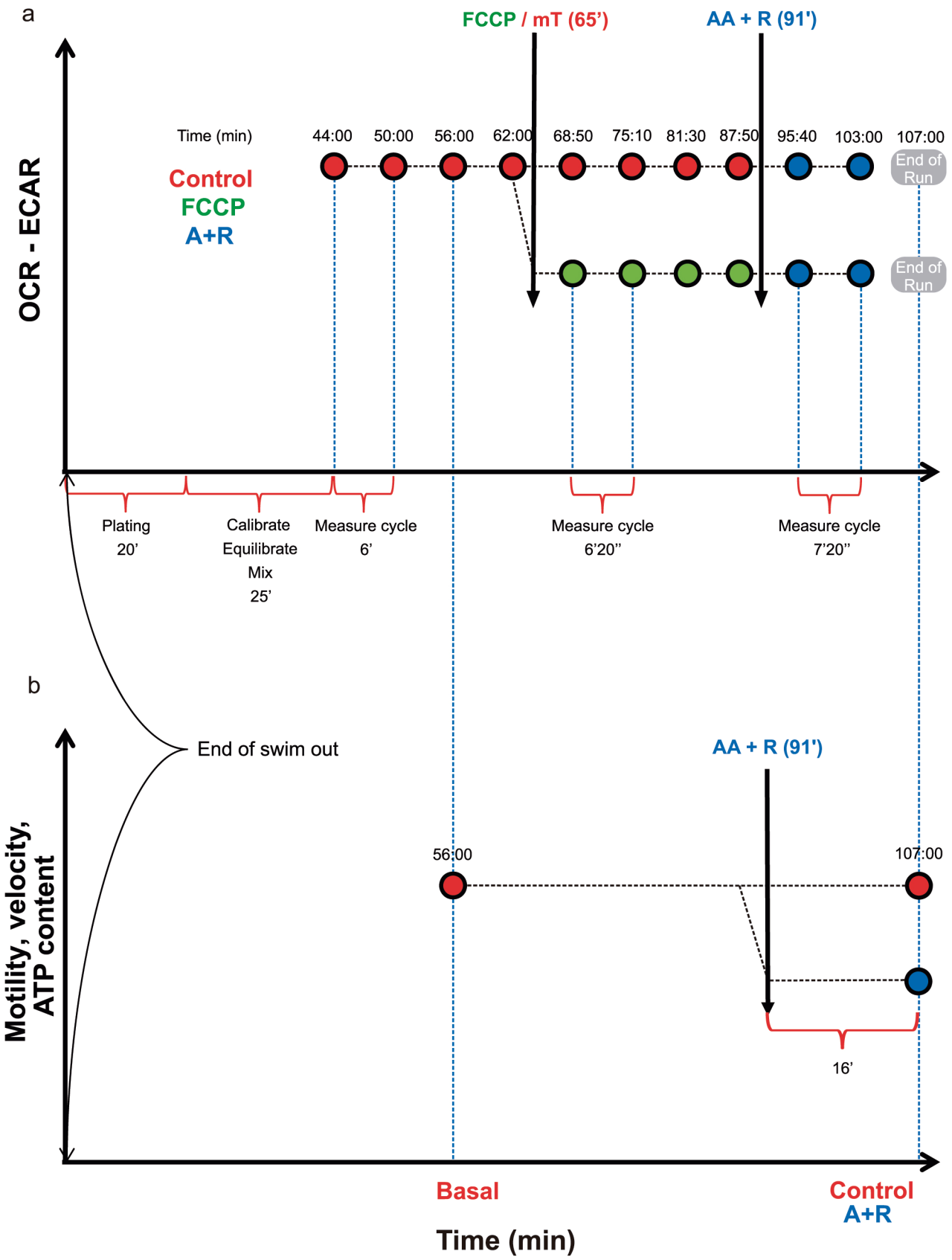
a
FCCP / mT (65')
AA + R (91')
OCR - ECAR
Time (min)
44:00
50:00
56:00
62:00
68:50
75:10
81:30
87:50
95:40
103:00
107:00
Control
FCCP
A+R
End of Run
End of Run
Plating
20'
Calibrate
Equilibrate
Mix
25'
Measure cycle
6'
Measure cycle
6'20"
Measure cycle
7'20"
b
End of swim out
AA + R (91')
Motility, velocity, ATP content
56:00
107:00
16'
Basal
Control
A+R
Time (min)

Figure 1

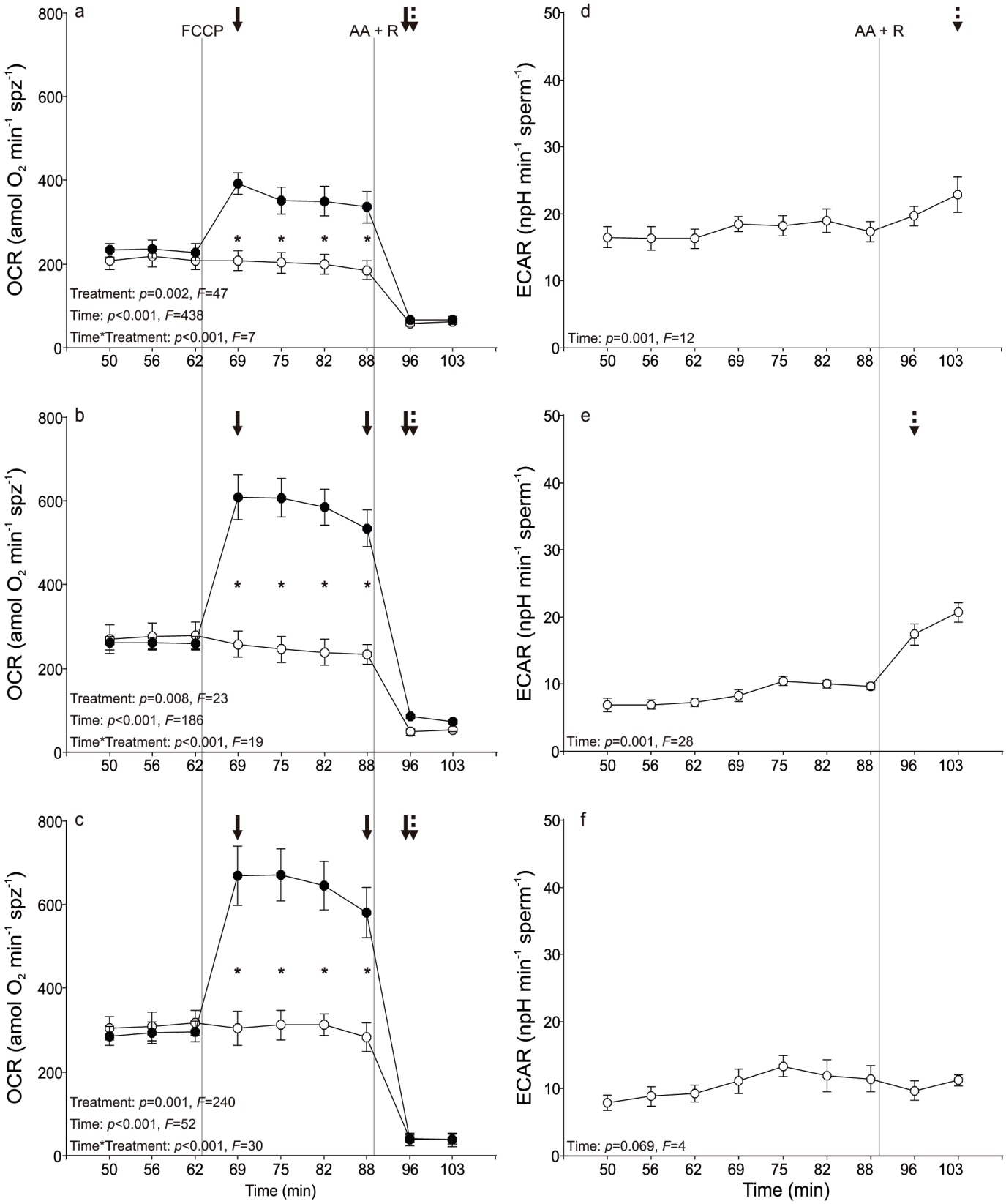
a
FCCP
AA + R
OCR (amol O2 min-1 spz-1)
Treatment: p=0.002, F=47
Time: p<0.001, F=438
Time*Treatment: p<0.001, F=7
d
AA + R
ECAR (npH min-1 sperm-1)
Time: p=0.001, F=12
b
OCR (amol O2 min-1 spz-1)
Treatment: p=0.008, F=23
Time: p<0.001, F=186
Time*Treatment: p<0.001, F=19
e
ECAR (npH min-1 sperm-1)
Time: p=0.001, F=28
c
OCR (amol O2 min-1 spz-1)
Treatment: p=0.001, F=240
Time: p<0.001, F=52
Time*Treatment: p<0.001, F=30
Time (min)
f
ECAR (npH min-1 sperm-1)
Time: p=0.069, F=4
Time (min)

Figure 2

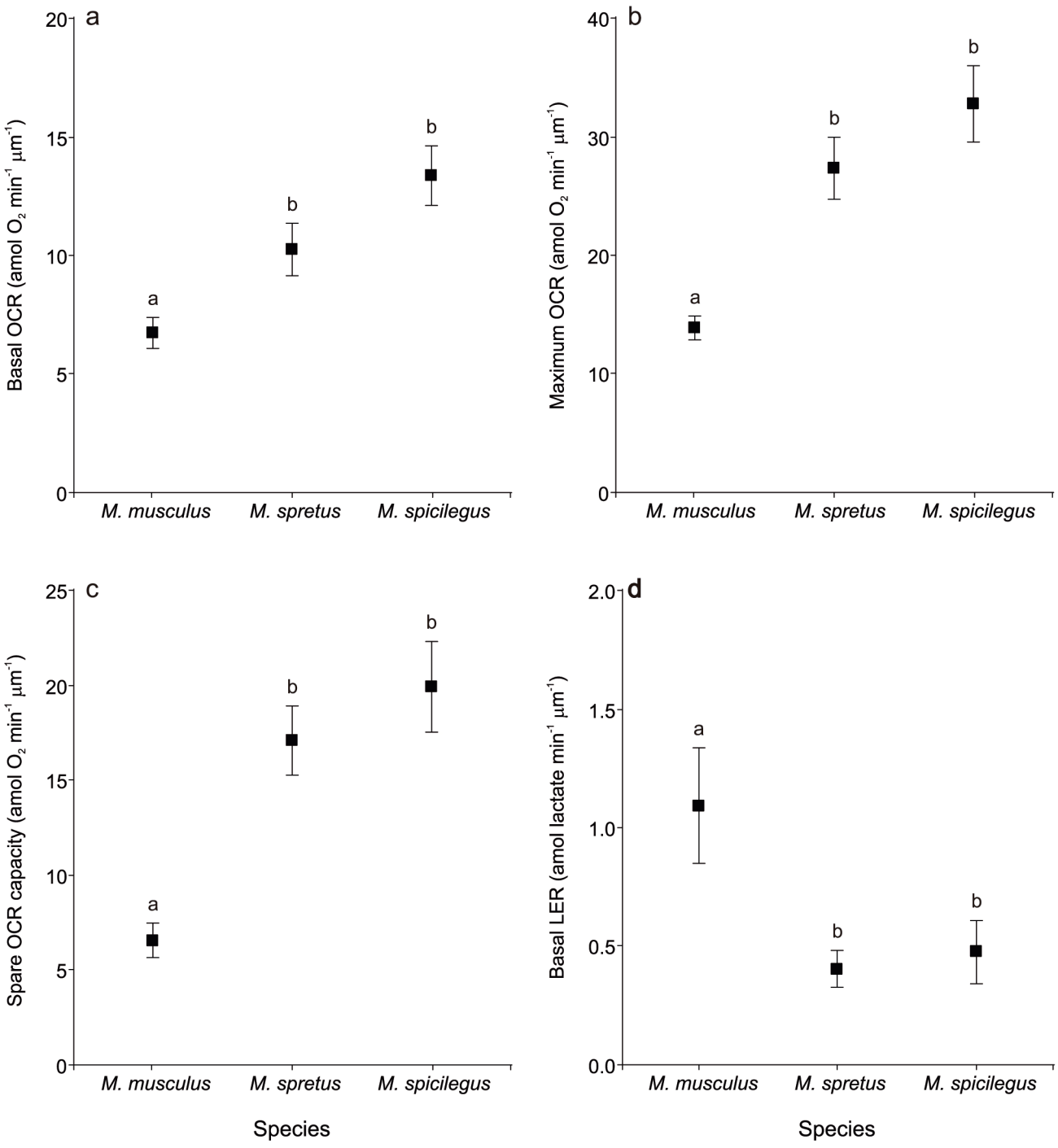
a
Basal OCR (amol O_2 min^{-1} μm^{-1})
20
15
10
5
0
a
b
b
M. musculus
M. spretus
M. spicilegus
b
Maximum OCR (amol O_2 min^{-1} μm^{-1})
40
30
20
10
0
a
b
b
M. musculus
M. spretus
M. spicilegus
c
Spare OCR capacity (amol O_2 min^{-1} μm^{-1})
25
20
15
10
5
0
a
b
b
M. musculus
M. spretus
M. spicilegus
Species
d
Basal LER (amol lactate min^{-1} μm^{-1})
2.0
1.5
1.0
0.5
0.0
a
b
b
M. musculus
M. spretus
M. spicilegus
Species

Figure 3

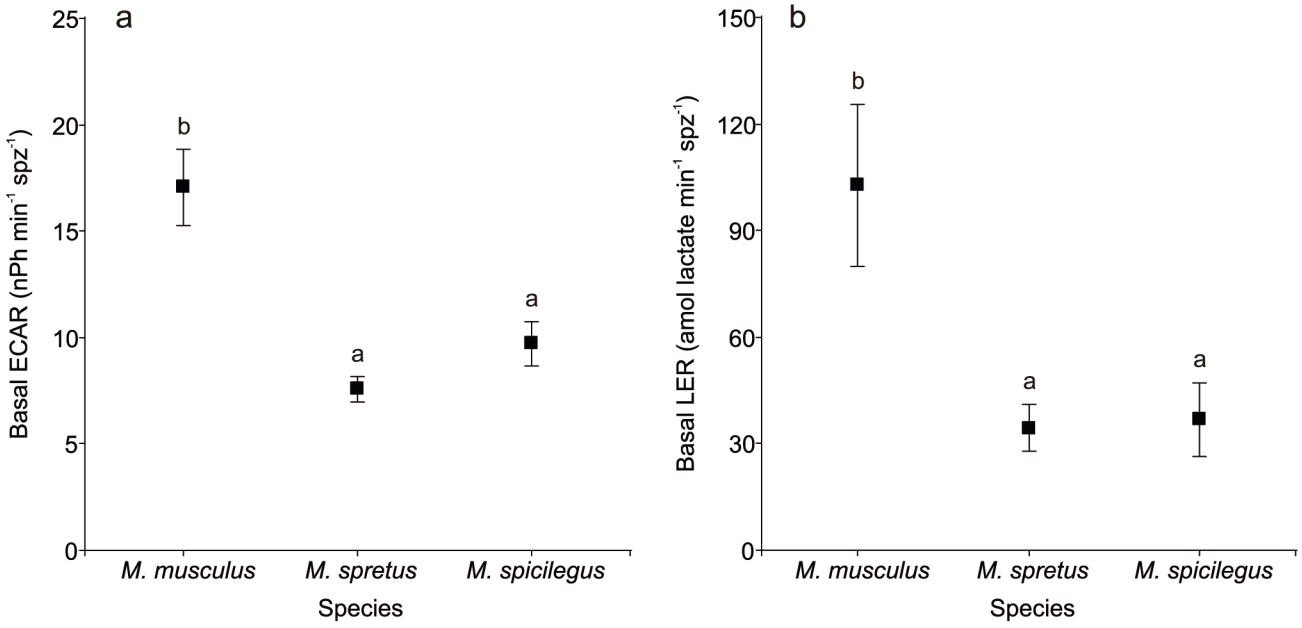
a
Basal ECAR (nPh min-1 spz-1)
25
20
15
10
5
0
b
a
a
M. musculus
M. spretus
M. spicilegus
Species
b
Basal LER (amol lactate min-1 spz-1)
150
120
90
60
30
0
b
a
a
M. musculus
M. spretus
M. spicilegus
Species

Figure 4

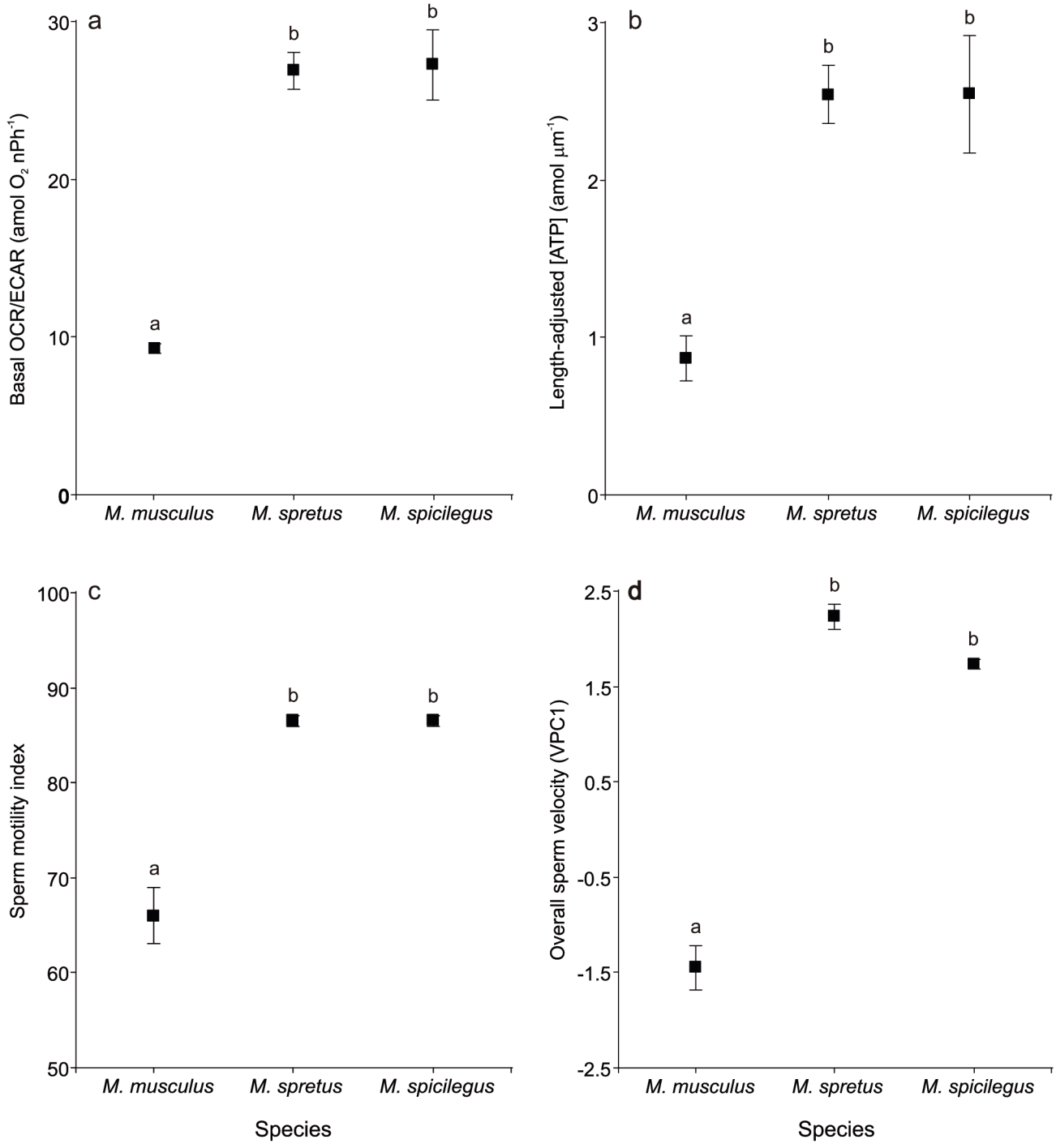
a
b
b
a
30
20
10
0
Basal OCR/ECAR (amol O_2 nPh^{-1})
M. musculus
M. spretus
M. spicilegus
b
a
b
b
3
2
1
0
Length-adjusted [ATP] (amol μm^{-1})
M. musculus
M. spretus
M. spicilegus
c
a
b
b
100
90
80
70
60
50
Sperm motility index
M. musculus
M. spretus
M. spicilegus
Species
d
a
b
b
2.5
1.5
0.5
-0.5
-1.5
-2.5
Overall sperm velocity (VPC1)
M. musculus
M. spretus
M. spicilegus
Species

Figure 5

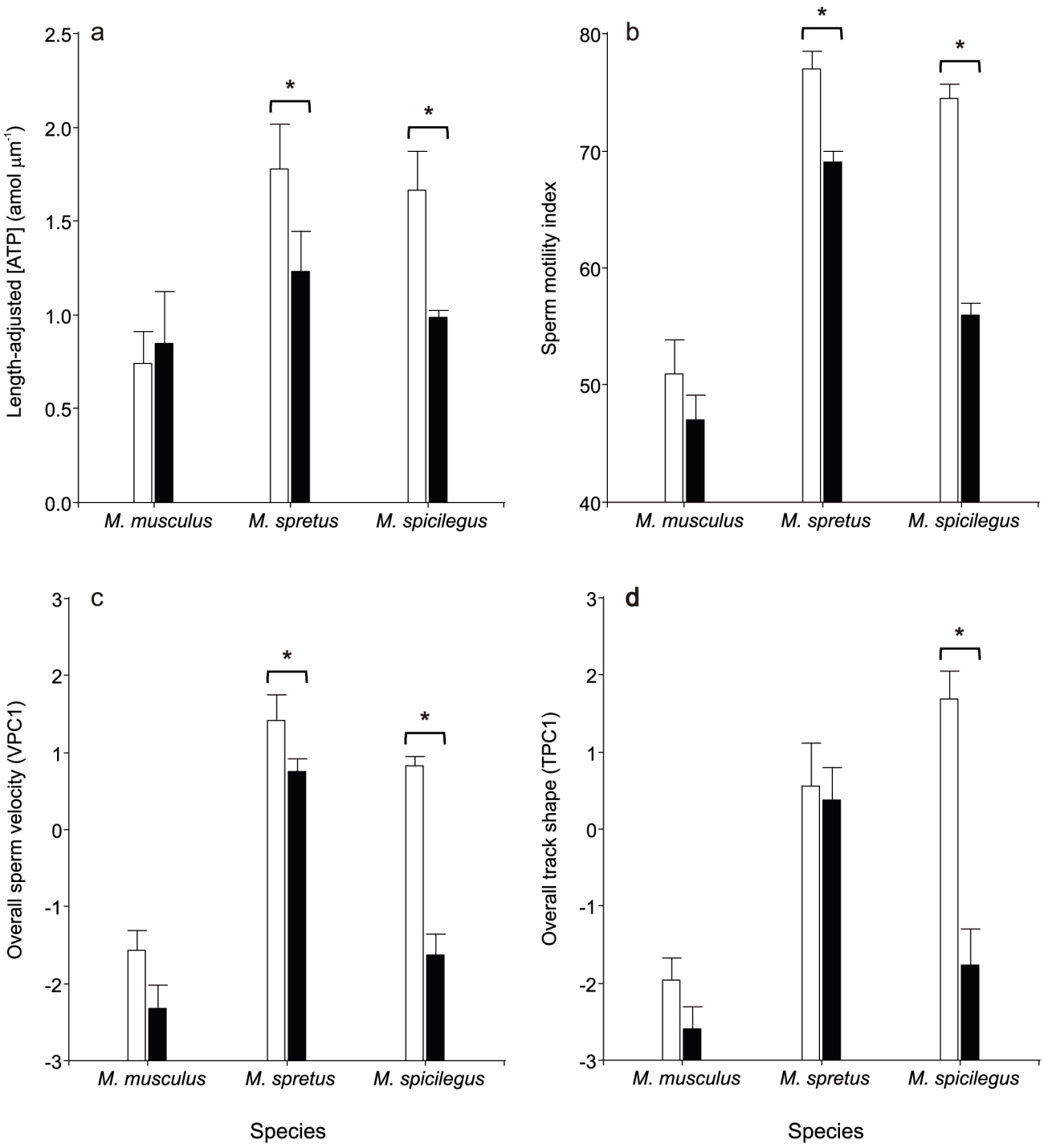
a
Length-adjusted [ATP] (amol µm-1)
2.5
2.0
1.5
1.0
0.5
0.0
*
*
M. musculus
M. spretus
M. spicilegus
b
Sperm motility index
80
70
60
50
40
*
*
M. musculus
M. spretus
M. spicilegus
c
Overall sperm velocity (VPC1)
3
2
1
0
-1
-2
-3
*
*
M. musculus
M. spretus
M. spicilegus
Species
d
Overall track shape (TPC1)
3
2
1
0
-1
-2
-3
*
M. musculus
M. spretus
M. spicilegus
Species

Figure 6

Bioenergetics:

Differences in ATP Generation Via Glycolysis and Oxidative Phosphorylation, and Relationships with Sperm Motility, in Mouse Species

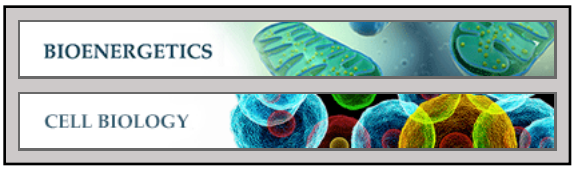

Maximiliano Tourmente, Pilar Villar-Moya, Eduardo Rial and Eduardo R. S. Roldan

J. Biol. Chem. published online June 5, 2015

Access the most updated version of this article at doi: 10.1074/jbc.M115.664813

This article cites 0 references, 0 of which can be accessed free at
http://www.jbc.org/content/early/2015/06/05/jbc.M115.664813.full.html#ref-list-1